JOURNAL OF GUIDANCE, CONTROL, AND DYNAMICS
Vol. 24, No. 6, November–December 2001

Capture Set Computation of an Optimally Guided Missile

Tuomas Raivio*
Helsinki University of Technology, FIN-02015 Espoo, Finland

A game theoretical approach is presented for numerically computing the capture set of an optimally guided medium-range air-to-air missile against a given target. Realistic point mass models are used because long flight times prevent simplifications such as coplanarity or constant speed target. The capture set is obtained by constructing saddle point trajectories on its boundary, or the barrier, numerically. Instead of solving a game of kind, the trajectories are identified by setting up an auxiliary game of degree. The necessary conditions of the auxiliary game are shown to coincide with those of the game of kind. The game of degree is solved from systematically varied initial states with a decomposition method that does not require setting up or solving the necessary conditions. Examples are calculated for a generic fighter and a missile.

Introduction

A MISSILE is generally designed to be faster and more agile than any aircraft. This kinematical advantage of a missile is, however, only temporary due to a finite and relatively short burn time of its rocket motor. In the coasting phase, the kinetic energy of the missile is rapidly dissipated by the aerodynamic drag force. In contrast to a missile, an aircraft can maintain its velocity as long as it has any fuel left. The asymmetry means that a missile does not necessarily reach the aircraft from an arbitrary launch position, but only from within a finite shooting range. The range depends on many factors, such as the performance and initial energy of the missile and target, the guidance law of the missile, the geometry of the shoot, and, moreover, on the maneuvering of the target. The set of launch positions that are inescapeable for the target is called the capture set (for example, see Ref. 1), or the no-escape envelope (Ref. 2). An estimate of the capture set is crucial, for example, in assessing the threat related to each opponent in an air combat and, furthermore, in considering actions to be taken. On the other hand, the unit cost of a single missile is usually significant, which calls for minimizing the number of premature shoots.

A worst-case estimate for the capture set with given vehicle models can be obtained by assuming that the missile uses a guidance law that produces the largest possible capture set. The situation can then be modeled as a pursuit–evasion game of kind (see Refs. 3 and 4), where the missile is identified with the pursuer and the aircraft with the evader. The aim in a game of kind is to identify the set of those initial states from which the optimally behaving pursuer can enforce a capture against any action of the evader. This paper presents a computational method to determine numerically solutions to the game of kind for adversary missile–aircraft encounters with realistic point mass models.

If the missile is assumed to use a known, perhaps nonoptimal, feedback guidance law, the capture set can be found via optimization of the evader's actions. Imado and Miwa[5,6] and Imado[7] have studied maneuvers that lead to a largest possible miss distance against missiles employing either proportional navigation (PN) or augmented PN. Shinar and Guelman[8] present a similarly optimal evasion strategy against a short-range PN missile with a simplified model, whereas Ong and Pierson[9] study optimal evasion of a surface-to-air PN missile with a slightly simplified model. Although some of the papers deal with quantitative evasion strategies, the results can be used in assessing the largest effective shooting distance as well.

Nevertheless, a general tendency seems to be toward better guidance schemes because most existing feedback laws are nonoptimal with excessive target maneuvers,[10,11] long launch distances,[12] and large initial deviations from the collision course.[1] If the guidance law of the missile is unknown, pursuit–evasion games provide a possibility to estimate the capture set under the worst-case assumption on the guidance law of the missile.

Isaacs[3] provides a unified procedure for solving a pursuit–evasion game of kind by identifying the barrier, a surface that envelops the initial states leading to a capture. Shinar et al.[1] and Green et al.[13] apply the approach of Isaacs to a simplified short-range missile scenario. Le Menec and Bernhard[14] use a similar model for barrier computation in an expert system for air combat. To allow solutions in closed form, the models assume coplanarity of the players and constant velocity of the evader. Unfortunately, these assumptions lose their validity as the duration of the encounter increases.

For game models that do not allow analytical solutions, a numerical solution scheme is needed. Grimm and Schaeffer[2] approximate the barrier by assuming more realistic vehicle models, but a near optimal feedback control for the evader, and optimize the farmost point from which a capture is still possible. Breitner et al.[15,16] have investigated the determination of the barrier with slightly simplified point mass models in the vertical plane. The approach is based on the numerical solution of the necessary conditions of the saddle point trajectories on the barrier.

In this paper, we consider rather realistically modeled flight vehicles maneuvering in three dimensions. Instead of solving the necessary conditions of a game of kind, we construct an auxiliary game of degree with the shooting range as the payoff and show that the open-loop representation of a feedback saddle point solution of this game satisfies the necessary conditions of a barrier saddle point trajectory. This is equivalent with the fact that the initial state obtained by solving the auxiliary game of degree lies on the barrier.

Points on a submanifold of the barrier, corresponding to partly fixed initial states of the players, are obtained by varying the initial geometry of the encounter and by repeatedly solving the auxiliary game of degree by a numerical decomposition method introduced in Ref. 17. In Ref. 18, the method is interpreted in a bilevel programming framework, the conditions for its convergence are stated, and the method is applied to a complex missile–aircraft pursuit–evasion game of degree. Comparison of the solutions with those obtained via an indirect approach shows an excellent agreement. In Ref. 19, the method is applied to a pursuit–evasion game modeling the visual identification procedure of an unknown aircraft.

The main advantage of this method is that the solution is obtained without explicitly stating or solving the necessary conditions of a saddle point. Instead, two optimal control problems are solved iteratively using discretization and nonlinear programming, until the saddle point has been found. Hence, the method offers an easy and rapid treatment of complex game models. To the author's knowledge, three-dimensional capture set computation with present models has not been reported earlier.

Received 18 November 1999; revision received 30 October 2000; accepted for publication 13 November 2000.

*Assistant Professor, P.O. Box 1100, Systems Analysis Laboratory; tuomas.raivio@hut.fi.

The paper is organized as follows: First, the dynamics of the players are introduced. The game of kind is then formulated, the necessary conditions of a barrier trajectory are briefly given, and the barrier submanifolds of interest are described. Next, the auxiliary game of degree is formulated, and it is shown that a solution to the auxiliary game satisfies the necessary conditions of a barrier trajectory. The decomposition method for the game of degree is presented before numerical examples and concluding remarks.

Game Dynamics

In the following, the missile is identified with the pursuer P and the aircraft with the evader E. Both P and E maneuver in three dimensions. We make the following simplifying assumptions:

1) The thrust and the drag forces, as well as the velocity vectors, are assumed parallel with the reference line of the vehicles.
2) The lift force is assumed to be orthogonal to the velocity vector and to point upward in the frame of reference of either vehicle.
3) The inertias of the flight vehicles are assumed negligible.
4) The coordinate frame assumes a flat Earth.

Then, the equations of motion are

$$\dot{x}_i = v_i \cos\gamma_i \cos\chi_i \tag{1}$$

$$\dot{y}_i = v_i \cos\gamma_i \sin\chi_i \tag{2}$$

$$\dot{h}_i = v_i \sin\gamma_i \tag{3}$$

$$\dot{\gamma}_i = \frac{g}{v_i}(n_i \cos\mu_i - \cos\gamma_i) \tag{4}$$

$$\dot{\chi}_i = \frac{g}{v_i}\frac{n_i \sin\mu_i}{\cos\gamma_i}, \qquad i = P, E \tag{5}$$

$$\dot{v}_P = \frac{1}{m_P(t)}\{T_P(t) - D_P[h_P, v_P, M(h_P, v_P), n_P]\} - g\sin\gamma_P \tag{6}$$

$$\dot{v}_E = \frac{1}{m_E}\{\eta_E T_{E,\max}[h_E, M(h_E, v_E)] - D_E[h_E, v_E, M(h_E, v_E), n_E]\} - g\sin\gamma_E \tag{7}$$

The state of the game is described by the state vector

$$z = [z_P', z_E']' = [x_P, y_P, h_P, \gamma_P, \chi_P, v_P, x_E, y_E, h_E, \gamma_E, \chi_E, v_E]' \tag{8}$$

The subscripts P and E refer to the pursuer and evader, respectively, and the prime denotes a transpose. The state variables x_i, y_i, h_i, γ_i, χ_i, and v_i, $i = P, E$, are the x and y coordinates, altitudes, flight-path angles, heading angles, and velocities of the players. The term shooting range that is used throughout the paper refers to the quantity $\{[x_P(0) - x_E(0)]^2 + [y_P(0) - y_E(0)]^2\}^{1/2}$, that is, the initial distance of the players in the xy plane.

The flight direction of the vehicles is controlled with the load factors n_P and n_E and the bank angles μ_P, $\mu_E \in [-\pi, \pi]$. The velocity of E is controlled by the throttle setting $\eta_E \in [0, 1]$ that selects the fraction of the maximal available thrust force $T_{E,\max}[h, M(h, v)]$, where M is the Mach number. The pursuer's thrust force $T_P(t)$ is in general a fixed function of time that cannot be controlled. The masses of the vehicles are denoted by m_P and m_E and the gravitational acceleration by g.

The drag forces of E and P are assumed to obey a quadratic polar (we suppress the subscripts for brevity),

$$D[h, v, M(h, v), n] = C_{D_0}[M(h, v)]Sq(h, v) + n^2 C_{D_l}[M(h, v)]\frac{(mg)^2}{Sq(h, v)} \tag{9}$$

where $C_{D_0}(\cdot)$ and $C_{D_l}(\cdot)$ are the zero drag and induced drag coefficients, S is the reference wing area, and $q(h, v) = 1/2\varrho(h)v^2$ is the dynamic pressure. The air density $\varrho(h)$ and the Mach number are computed using the international standard atmosphere.

The load factors n_P and n_E cannot be chosen freely. At low velocities, a large load factor requires a large angle of attack, which results in loss of lift force and stall. At higher velocities, the magnitudes of the load factors are constrained by the largest accelerations that the flight vehicles and the pilot tolerate. Here, the bounds are approximated by the box constraints

$$n_P \in [0, n_{P,\max}] \tag{10}$$

$$n_E \in [0, n_{E,\max}] \tag{11}$$

To summarize, we require that the players' control vectors $\boldsymbol{u}_P(t)$ and $\boldsymbol{u}_E(t)$ satisfy

$$\boldsymbol{u}_P(t) := [n_P(t), \mu_P(t)]' \in S_P := [0, n_{P,\max}] \times [-\pi, \pi] \tag{12}$$

$$\boldsymbol{u}_E(t) := [n_E(t), \mu_E(t), \eta_E(t)]' \in S_E := [0, n_{E,\max}] \times [-\pi, \pi] \times [0, 1] \tag{13}$$

In addition, the players have to stay in their flight envelopes. For the evader, the boundaries of interest are the minimum altitude constraint

$$h_E \geq h_{E,\min} \tag{14}$$

and the dynamic pressure constraint

$$q(h_E, v_E) \leq q_{E,\max} \tag{15}$$

The pursuer must obey the minimum altitude constraint

$$h_P \geq h_{P,\min} \tag{16}$$

Game of Kind

Let us assume that the players, obeying Eqs. (1–7) and (12–16) have perfect information on the state of the game. In the game of kind, as defined by Isaacs,[3] the objective of the pursuer is to enforce the capture, whereas the objective of the evader is to avoid it. A capture occurs when $z(t)$ enters a target set Λ. In this paper, Λ is defined as a set of points where the distance of the players is smaller than a given capture radius d. The boundary $\partial\Lambda$ of Λ is given by the terminal manifold or capture condition

$$l[z_P(T), z_E(T)] = [x_P(T) - x_E(T)]^2 + [y_P(T) - y_E(T)]^2 + [h_P(T) - h_E(T)]^2 - d^2 = 0 \tag{17}$$

The capture condition also implicitly specifies the terminal time T. The solution of a game of kind is the set of all admissible initial conditions $z(0) = z_0$ from which the pursuer can achieve the capture against any admissible control of the evader. If there exists another set of initial states from which the pursuer cannot enforce the capture, the two sets (excluding the interior of Λ) are separated by a piecewise continuously differentiable hypermanifold called the barrier. The barrier is a collection of saddle point solution trajectories, also termed as barrier trajectories, that satisfy

$$\max_{\boldsymbol{u}_E}\min_{\boldsymbol{u}_P}\frac{\mathrm{d}}{\mathrm{d}t}l[z(T)] = 0 \tag{18}$$

(see Refs. 3 and 15). An infinitesimal change of the initial state or a deviation of either player from the optimal strategy on the barrier immediately results in a capture or escape. Instead of an exhaustive search in the state space, the game of kind can be solved by determining the barrier, or equivalently, the saddle point trajectories forming it.

Note that in the present problem the functional limits of the missile can give rise to additional capture set boundaries. For example, a proximity fuse may require a certain minimum launch distance. These boundaries, however, are not explored here.

Necessary Conditions of a Barrier Trajectory

The necessary conditions, satisfied by a barrier trajectory, consist of the 1) equations of motion, 2) control and state variable inequality constraints, 3) optimal controls of the players that minimaximize the Hamiltonian of the game at each time instant, 4) adjoint differential equations, 5) interior point conditions for the transitions from one solution arc to another, 6) jump conditions for the adjoint trajectories at some of the transitions, 7) terminal condition, and 8) initial values of the state variables and final conditions for the adjoint variables.

The initial state is selected so that condition (18) holds. The final conditions of the adjoint variables are given as

$$\boldsymbol{\lambda}(T^*) = \alpha \frac{\partial}{\partial \boldsymbol{z}} l[\boldsymbol{z}^*(T^*)] \tag{19}$$

where $\boldsymbol{\lambda}(t)$ is the adjoint vector, α is a positive multiplier, and the asterisk denotes a saddle point solution trajectory that results when both players apply their optimal saddle point strategies.

For the game at hand, the condition (1) is given by Eqs. (1–7), condition (2) by Eqs. (12–16), and condition (7) by Eq. (17). The explicit form of conditions (3–6) is not needed here, but can be found, for example, in Ref. 20 and the literature cited therein. Condition (18) gives

$$\frac{\mathrm{d}}{\mathrm{d}t} l[\boldsymbol{z}^*(T^*)] = \frac{\partial l}{\partial z}[\boldsymbol{z}^*(T^*)] \cdot \dot{\boldsymbol{z}}^*(T^*) = 0 \tag{20}$$

Differentiating $l(\cdot)$, given by Eq. (17), and substituting the relevant components of $\dot{z}(t)$, given by Eqs. (1–3), result in the following constraint for the final flight-path angles, heading angles, and the velocities of the players (we suppress the asterisks for brevity):

$$v_P(T) = v_E(T) \frac{\Delta x \cos\gamma_E(T)\cos\chi_E(T) + \Delta y \cos\gamma_E(T)\sin\chi_E(T) + \Delta h \sin\gamma_E(T)}{\Delta x \cos\gamma_P(T)\cos\chi_P(T) + \Delta y \cos\gamma_P(T)\sin\chi_P(T) + \Delta h \sin\gamma_P(T)} \tag{21}$$

where $\Delta x = x_P(T) - x_E(T)$, $\Delta y = y_P(T) - y_E(T)$, and $\Delta h = h_P(T) - h_E(T)$. The final conditions of the adjoint variables (19) yield

$$\lambda_{x_P}(T^*) = -\lambda_{x_E}(T^*) = 2\alpha\left[x_P^*(T^*) - x_E^*(T^*)\right] \tag{22}$$

$$\lambda_{y_P}(T^*) = -\lambda_{y_E}(T^*) = 2\alpha\left[y_P^*(T^*) - y_E^*(T^*)\right] \tag{23}$$

$$\lambda_{h_P}(T^*) = -\lambda_{h_E}(T^*) = 2\alpha\left[h_P^*(T^*) - h_E^*(T^*)\right] \tag{24}$$

In addition,

$$\lambda_{v_P}(T^*) = \lambda_{v_E}(T^*) = 0 \tag{25}$$

$$\lambda_{\gamma_P}(T^*) = \lambda_{\gamma_E}(T^*) = 0 \tag{26}$$

$$\lambda_{\chi_P}(T^*) = \lambda_{\chi_E}(T^*) = 0 \tag{27}$$

because the corresponding state variables are free at $t = T^*$.

Barrier Submanifolds

In principle, the barrier could be identified by integrating the necessary conditions (1–8) backward in time, starting from the transversality conditions (22–27) and every point satisfying condition (18) on $\partial\Lambda$ (Ref. 3). Nevertheless, the barrier is an 11-dimensional hypermanifold in the 12-dimensional state space, and its construction as such would be a formidable task. Besides, many initial states, like the ones where the pursuer is initially heading away from the evader, hardly bear any practical significance. Therefore, we concentrate on a submanifold of the barrier.

Because the atmosphere is assumed laterally homogenous, we fix

$$x_E(0) = y_E(0) = 0 \tag{28}$$

For the same reason, we can fix

$$y_P(0) = 0 \tag{29}$$

and let $\chi_E(0)$ vary. Consequently, the shooting range is simply given by $x_P(0)$. Because we anticipate long solution times, transients related to the initial flight-path angle of the evader are considered negligible, and we use

$$\gamma_E(0) = 0 \tag{30}$$

To further decrease the dimension, we fix the initial velocity and altitude of the evader and the initial velocity of the pursuer:

$$v_E(0) = v_{E,0},\ h_E(0) = h_{E,0} \tag{31}$$

$$v_P(0) = v_{P,0} \tag{32}$$

In the computations they will be treated as parameters. Finally, we let the pursuer select its initial flight-path angle and heading angle freely,

$$\gamma_P(0) = \gamma_P^*(0) \tag{33}$$

$$\chi_P(0) = \chi_P^*(0) \tag{34}$$

Conventionally, one would assume that at the moment of the launch the target has to be in the visual field of the missile's sensor mechanisms, dictated by the initial direction of the missile. This would give rise to an initial condition of the form

$$k[x_P(0), h_P(0), \gamma_P(0), \chi_P(0)] \le 0 \tag{35}$$

Nevertheless, because most long-range missiles nowadays can download midcourse navigation information from an aircraft that is even not necessarily the launching one, constraining is considered unnecessary. The additional necessary conditions corresponding to Eqs. (33) and (34) are

$$\lambda_{\gamma P}(0) = \lambda_{\chi P}(0) = 0 \tag{36}$$

The resulting submanifold of the barrier lies in the intersection of the hyperplanes (28–32) and the manifolds (33) and (34) and is two dimensional. It specifies the maximal shooting range $x_P^*(0) > 0$ as a function of the initial geometry described by $h_P(0)$ and $\chi_E(0)$. To determine the $x_P^*(0)$ corresponding to $h_P(0) = h_{P,0}$ and $\chi_E(0) = \chi_{E,0}$, one could, for example, solve the multipoint boundary value problem resulting from the necessary conditions (1–8) numerically (see Refs. 15 and 16). In the following, however, we develop an alternative approach that utilizes the decomposition method described in Ref. 17.

Auxiliary Game of Degree

That the total impulse of the missile is finite allows one to set up a game of degree with the shooting range as the payoff. Let us, in addition to Eqs. (28–32), fix also $h_P(0) = h_{P,0}$ and $\chi_E(0) = \chi_{E,0}$. Consider then the game

$$\max_{\boldsymbol{u}_E} \min_{\boldsymbol{u}_P, x_P(0), \gamma_P(0), \chi_P(0)} -\kappa\xi(T) \tag{37}$$

$$\dot{\boldsymbol{z}}_P = \boldsymbol{f}_P(\boldsymbol{z}_P, \boldsymbol{u}_P, t)$$

$$\boldsymbol{z}_P(0) = [x_P(0), 0, h_{P,0}, v_{P,0}, \gamma_P(0), \chi_P(0)]' \tag{38}$$

$$\dot{\boldsymbol{z}}_E = f_E(z_E, u_E), \qquad \boldsymbol{z}_E(0) = [0, 0, h_{E,0}, v_{E,0}, 0, \chi_{E,0}]' \tag{39}$$

$$\dot{\xi} = 0, \qquad \xi(0) = x_P(0) \tag{40}$$

$$\boldsymbol{u}_E(t) \in S_E, \qquad \boldsymbol{u}_P(t) \in S_P \tag{41}$$

$$h_E(t) \ge h_{E,\min}, \qquad h_P(t) \ge h_{P,\min} \tag{42}$$

$$q[h_E(t), v_E(t)] \le q_{\max} \tag{43}$$

$$l[z(T)] = 0 \tag{44}$$

The payoff is always negative because the scaling factor κ is positive. The dummy state $\xi(t)$ is introduced to transform the initial state payoff into a theoretically more sound terminal state cost function. The absolute value of $\xi(T)$ equals the shooting range. The state equations (38) and (39) are as in Eqs. (1–7).

We now postulate that a solution that satisfies the necessary conditions of a saddle point of the auxiliary game of degree also satisfies the necessary conditions of a barrier trajectory. Checking this is straightforward for the items 1–7 on the list in the preceding section, assuming that the switching structure of the solution of the game of degree coincides with that of the barrier trajectory associated with the computed initial state. For item 8, we note the following. The final conditions of the adjoint variables in the game of degree are

$$\mu_{x_P}(\tilde{T}) = -\mu_{x_E}(\tilde{T}) = 2\beta[\tilde{x}_P(\tilde{T}) - \tilde{x}_E(\tilde{T})] \tag{45}$$

$$\mu_{y_P}(\tilde{T}) = -\mu_{y_E}(\tilde{T}) = 2\beta[\tilde{y}_P(\tilde{T}) - \tilde{y}_E(\tilde{T})] \tag{46}$$

$$\mu_{h_P}(\tilde{T}) = -\mu_{h_E}(\tilde{T}) = 2\beta[\tilde{h}_P(\tilde{T}) - \tilde{h}_E(\tilde{T})] \tag{47}$$

$$\mu_{v_P}(\tilde{T}) = \mu_{v_E}(\tilde{T}) = 0 \tag{48}$$

$$\mu_{\gamma_P}(\tilde{T}) = \mu_{\gamma_E}(\tilde{T}) = 0 \tag{49}$$

$$\mu_{\chi_P}(\tilde{T}) = \mu_{\chi_E}(\tilde{T}) = 0 \tag{50}$$

$$\mu_{\xi}(\tilde{T}) = -\kappa \tag{51}$$

where $\boldsymbol{\mu}(t)$ is the adjoint vector and $(\tilde{\ })$ refers to the solution of the game of degree. Conditions (45–50) coincide with conditions (22–27). Obviously, $\mu_{\gamma_E}(0) = \mu_{\chi_E}(0) = 0$, which yields condition (36). Note that condition (51) is not totally decoupled; by the use of calculus of variations, it is rather easy to show that the initial condition (40) implies $\mu_{\xi}(0) = -\mu_{x_P}(0)$. Because both $\mu_{\xi}(t)$ and $\mu_{x_P}(t)$ are constant, $\mu_{\xi}(\tilde{T}) = -\kappa = -\mu_{x_P}(\tilde{T})$. On the other hand, $\mu_{x_P}(\tilde{T})$ should satisfy condition (45). Nevertheless, as long as $\tilde{x}_P(\tilde{T}) > \tilde{x}_E(\tilde{T})$, then $\kappa > 0$ can be selected freely without affecting the solution. In the computations of this paper the assumption holds.

Finally, substituting Eqs. (45–51) to the necessary condition

$$\begin{aligned}\tilde{H}[\tilde{\boldsymbol{z}}(\tilde{T}), \tilde{\boldsymbol{u}}_P(\tilde{T}), \tilde{\boldsymbol{u}}_E(\tilde{T}), \boldsymbol{\mu}(\tilde{T}), \tilde{\xi}(\tilde{T}), \tilde{T}] \\ \doteq \boldsymbol{\mu}'(\tilde{T})\{\boldsymbol{f}_P[\tilde{\boldsymbol{z}}_P(\tilde{T}), \tilde{\boldsymbol{u}}_P(\tilde{T}), \tilde{T}]', \boldsymbol{f}_E[\tilde{\boldsymbol{z}}_E(\tilde{T}), \tilde{\boldsymbol{u}}_E(\tilde{T})]'\}' \\ + \mu_{\xi}(\tilde{T}) \cdot 0 = 0\end{aligned} \tag{52}$$

of the game of degree and canceling the common factor $\beta > 0$ show that $\tilde{\boldsymbol{z}}(\tilde{T})$ satisfies condition (21). This concludes that $\tilde{\boldsymbol{z}}(t), t \in [0, \tilde{T}]$, satisfies the necessary conditions of a barrier trajectory. Especially the initial states $\tilde{\boldsymbol{z}}_P(0) = [\tilde{x}_P(0), 0, h_{P,0}, v_{P,0}, \tilde{\gamma}_P(0), \tilde{\chi}_P(0)]'$ and $\boldsymbol{z}_E(0) = [0, 0, h_{E,0}, v_{E,0}, 0, \chi_{E,0}]'$ belong to the barrier. Thus, the maximal shooting range $x_P^*(0)$ corresponding to $h_P(0) = h_{P,0}$ and $\chi_E(0) = \chi_{E,0}$ on the barrier submanifold defined earlier is given by $\tilde{x}_P(0)$. Parts of the submanifold can now be produced by systematically varying $h_P(0)$ and $\chi_E(0)$ and solving the game of degree (37–44) repeatedly. Different submanifolds are obtained by varying $v_{E,0}$, $h_{E,0}$, and $v_{P,0}$ in Eqs. (31) and (32). In this way, for example, the effect of the initial velocity of the evader on the shooting range can be assessed.

Solving the Game of Degree

The approach just presented is computationally intensive because the auxiliary game of degree has to be solved numerous times from different initial conditions. Indirect methods that solve the necessary conditions of a saddle point solution could be used, but the small domain of convergence and the need to specify the sequence of unconstrained, constrained, and singular solution arcs correctly in advance cause practical problems. Furthermore, the work needed in deriving the necessary conditions should not be underestimated (for an example, see Ref. 20).

A new solution method is presented in Ref. 17. It is based on the fact that, for games where the payoff is terminal and the state equation and the control as well as state variable inequality constraints are separable in players' control and state variables, the necessary conditions are coupled only at $t = T$ through the payoff and the capture condition. Obviously, the auxiliary game of the preceding section falls into this category. In the method, the solution of the necessary conditions is decomposed into two subproblems that are solved iteratively. The subproblems are optimal control problems, and in the end of the iteration, the necessary optimality conditions of these problems coincide with the necessary conditions of the saddle point solution.

The subproblems can be solved with any direct or indirect trajectory optimization approach. The actual motivation behind the decomposition is, however, that with a suitable discretization scheme the subproblems can be transformed into nonlinear programming problems. For a review of different discretization schemes, see Ref. 21. The necessary conditions are then not directly involved in the solution process, but the solution, together with the Lagrange multipliers of the problem, approximates the control, state, and adjoint trajectories with an accuracy that depends on the discretization grid and the order of the discretization method.

In the following we describe the method when applied to the preceding auxiliary game. From the computational point of view, the dummy state variable ξ is void. For clarity, we eliminate it and consider directly the minimaximization of $x_P(0)$.

Assume that the pursuit–evasion game admits a saddle point in feedback strategies. Then, an open-loop representation of a feedback saddle point trajectory can be computed by solving the maxmin problem

$$\max_{\boldsymbol{u}_E} \min_{\boldsymbol{u}_P, x_P(0), \gamma_P(0), \chi_P(0)} -x_P(0) \tag{53}$$

$$\dot{\boldsymbol{z}}_P = \boldsymbol{f}_P(\boldsymbol{z}_P, \boldsymbol{u}_P, t)$$

$$\boldsymbol{z}_P(0) = [x_P(0), 0, h_{P,0}, v_{P,0}, \gamma_P(0), \chi_P(0)]' \tag{54}$$

$$\dot{\boldsymbol{z}}_E = \boldsymbol{f}_E(\boldsymbol{z}_E, \boldsymbol{u}_E), \qquad \boldsymbol{z}_E(0) = [0, 0, h_{E,0}, v_{E,0}, 0, \chi_{E,0}]' \tag{55}$$

$$\boldsymbol{u}_E(t) \in S_E, \qquad \boldsymbol{u}_P(t) \in S_P \tag{56}$$

$$h_E(t) \ge h_{E,\min}, \qquad h_P(t) \ge h_{P,\min} \tag{57}$$

$$q[h_E(t), v_E(t)] \le q_{\max} \tag{58}$$

$$l[\boldsymbol{z}_P(T), \boldsymbol{z}_E(T)] = 0 \tag{59}$$

To obtain the maxmin solution, we set up an iteration, where the pursuer's minimization problem is solved with a fixed current trajectory of the evader. The evader's trajectory is then improved by a feasible step, and the process is repeated until convergence.

Let us first consider the pursuer's minimization problem

$$\min_{\boldsymbol{u}_P, x_P(0), \gamma_P(0), \chi_P(0), T} -x_P(0) \tag{60}$$

$$\dot{\boldsymbol{z}}_P = \boldsymbol{f}_P(\boldsymbol{z}_P, \boldsymbol{u}_P, t)$$

$$\boldsymbol{z}_P(0) = [x_P(0), 0, h_{P,0}, v_{P,0}, \gamma_P(0), \chi_P(0)] \tag{61}$$

$$\boldsymbol{u}_P(t) \in S_P, \qquad h_P(t) \ge h_{P,\min} \tag{62}$$

$$l\big[\boldsymbol{z}_P(T), \boldsymbol{z}_E^0(T)\big] = 0 \tag{63}$$

where $\boldsymbol{z}_E^0(t), t \ge 0$ is a fixed trajectory of the evader and $l(\cdot)$ is defined as in Eq. (17). Let the solution trajectory be $\bar{\boldsymbol{z}}_P(t)$ and the final time $\bar{T}$ and denote the capture point $\boldsymbol{z}_E^0(\bar{T})$ by $\bar{\boldsymbol{e}}$. Now, $\bar{\boldsymbol{z}}_P(t)$ is also an optimal trajectory for the problem where the evader's trajectory is

replaced by the fixed point $\bar{e}$ and the final time is fixed to $\bar{T}$. In the neighborhoodof$(\bar{e}, \bar{T})$ define

$$V(\boldsymbol{e}, T) = \min_{\boldsymbol{u}_P, x_P(0), \gamma_P(0), \chi_P(0)} \{-x_P(0) \mid \dot{\boldsymbol{z}}_P = \boldsymbol{f}_P(\boldsymbol{z}_P, \boldsymbol{u}_P, t), t \in [0, T], \boldsymbol{z}_P(0) = [x_P(0), 0, h_{P,0}, v_{P,0}, \gamma_P(0), \chi_P(0)], \boldsymbol{u}_P(t) \in S_P, h_P(t) \geq h_{P,\min}, l[\boldsymbol{z}_P(T), \boldsymbol{e}] = 0\} \tag{64}$$

The maxmin problem (37–44) is equivalent to maximizing $V(\boldsymbol{e}, T)$ subject to the evader's constraints. This problem is difficult to solve because $V(\cdot)$ cannot be expressed analytically. We, therefore, approximate the solution that maximizes Eq. (64) with a solution to the problem where the final time is fixed to $\bar{T}$, and $V(\boldsymbol{e}, \bar{T})$ is linearized in the neighborhood of $\bar{\boldsymbol{e}}$. This problem can be stated as

$$\max_{\boldsymbol{u}_E} \frac{\partial V}{\partial \boldsymbol{e}}(\bar{\boldsymbol{e}}, \bar{T})[\boldsymbol{z}_E(\bar{T}) - \bar{\boldsymbol{e}}] \tag{65}$$

$$\dot{\boldsymbol{z}}_E = \boldsymbol{f}_E(\boldsymbol{z}_E, \boldsymbol{u}_E), \qquad t \in [0, T], \qquad \boldsymbol{z}_E(0) = \boldsymbol{z}_{E0} \tag{66}$$

$$\boldsymbol{u}_E(t) \in S_E, \qquad h_E(t) \geq h_{E,\min}, \qquad q[h_E(t), v_E(t)] \leq q_{E,\max} \tag{67}$$

where the gradient is a row vector. Basic sensitivity results applied to V (see Refs. 17 and 18 and the references cited therein) imply that the gradient of V with respect to $\boldsymbol{e}$ at $(\bar{\boldsymbol{e}}, \bar{T})$ is given by the analytical expression

$$\frac{\partial}{\partial \boldsymbol{e}} V(\bar{\boldsymbol{e}}, \bar{T}) = \frac{-\partial}{\partial \boldsymbol{e}} x_P(0) + \bar{\alpha} \frac{\partial}{\partial \boldsymbol{e}} l[\bar{\boldsymbol{z}}_P(\bar{T}), \bar{\boldsymbol{e}}] = \bar{\alpha} \frac{\partial}{\partial \boldsymbol{e}} l[\bar{\boldsymbol{z}}_P(\bar{T}), \bar{\boldsymbol{e}}] \tag{68}$$

where $\bar{\alpha}$ is the Lagrange multiplier associated with the capture condition (63) in the solution of the minimization problem (60–63). In this game,

$$\frac{\partial}{\partial \boldsymbol{e}} l[\bar{\boldsymbol{z}}_P(\bar{T}), \bar{\boldsymbol{e}}] = -2\{[\bar{x}_P(\bar{T}) - \bar{x}_E(\bar{T})], [\bar{y}_P(\bar{T}) - \bar{y}_E(\bar{T})], [\bar{h}_P(\bar{T}) - \bar{h}_E(\bar{T})]\}' \tag{69}$$

Denote the solution trajectory of Eqs.(65–67) by $\boldsymbol{z}_E^1(t)$, $t \in [0, \bar{T}]$. Also denote $T^1 = \bar{T}$. One iteration is completed by extending $\boldsymbol{z}_E^1(t)$, for example, linearly as

$$\boldsymbol{z}_E^1(t) = \begin{cases} \boldsymbol{z}_E^1(t), & t \leq T^1 \\ \boldsymbol{z}_E^1(T^1) + \dot{\boldsymbol{z}}_E^1(T^1)(t - T^1) & t > T^1 \end{cases} \tag{70}$$

The extension is needed because, in general, if convergence has not yet been achieved, T^{k+1} can be larger than T^k. The extended solution is then inserted to the minimization problem (60–63), which is solved anew to locate the new capture point and to compute the linear approximation of $V(\cdot)$. The iteration is continued until the relative change in $V(\cdot)$ becomes less than a prescribed value. To summarize, the iteration proceeds as follows:

1) Fix an initial trajectory $\boldsymbol{z}_E^0(t)$, $t \geq 0$ of evader and solve problem (60–63). Obtain $\bar{\boldsymbol{z}}_P(t)$, $\bar{\boldsymbol{e}}$, $\bar{T}$, and $\bar{\alpha}$. Set $k := 1$.

2) Solve problem (65–67) using $\bar{\boldsymbol{e}}$, $\bar{T}$, and $\bar{\alpha}$ to obtain $\boldsymbol{z}_E^k(t)$.

3) Insert the extended solution $\boldsymbol{z}_E^k(t)$ of problem (65–67) into Eqs. (60–63) and solve to obtain $\bar{\boldsymbol{z}}_P(t)$, $\bar{\boldsymbol{e}}$, $\bar{T}$, and $\bar{\alpha}$. If the relative change of the payoff is smaller than the prescribed accuracy, terminate. Otherwise, set $k := k + 1$ and go to step 2.

In Ref. 17, it is shown that when the method converges, the solution satisfies the necessary conditions of an open-loop representation of a feedback saddle point on regular solution arcs and on such singular arcs that involve only one of the players. There are, however, certain singular surfaces, such as the equivocal surface (see Ref. 3), that involve both players and couple the necessary conditions before the termination of the game. These surfaces require additional necessary conditions to be satisfied that cannot be expressed as the optimality conditions of the subproblems. The maxmin solution then differs from the saddle point solution (see Ref. 17 and the discussion in Ref. 18). Although it is in practice impossible to prove exactly, we can rather safely assume that the solution of the present game does not involve such surfaces.

In the approach just described, the saddle point problem is first decomposed, and the subproblems are discretized. In Ref. 18, the saddle point problem is first discretized and then solved using a feasible direction method. The discretized problem is identified with a bilevel programming problem (see Ref. 22 and the references cited in Ref. 18) with the maximization as the upper level problem and the minimization as the lower level problem, and a feasible direction method with generally established convergence conditions is proposed for solving the bilevel programming problem. The feasible direction method turns out to be almost identical with the decomposition method presented here, which provides an alternative interpretation and conditions for the convergence of the decomposition method as well.

Numerical Examples

In the following, we compute parts of the submanifolds of the barrier corresponding to two initial altitudes and velocities of the evader and one initial velocity of the pursuer. We use a generic medium-range air-to-air missile model. The thrust force of the rocket motor is given by

$$T_P(t) = \begin{cases} T_B, & 0 \leq t \leq 3\,\text{s} \\ T_S, & 3 < t \leq 15\,\text{s} \\ 0, & t > 15\,\text{s} \end{cases} \tag{71}$$

Consequently, the mass of the missile first decreases piecewise linearly and remains then constant. The mass of the evader is assumed constant. The drag coefficients of both vehicles are approximated by rational polynomials on the basis of realistic tabular data. The data describing $T_{E,\max}[h_E, M(h_E, v_E)]$ is approximated by a two-dimensional polynomial. We set $n_{E,\max} = 7$, $n_{P,\max} = 20$, and $q_{E,\max} = 80$ kPa. The evader's data used in the numerical examples represent a high-performance fighter aircraft. For details, see literature cited in Ref. 20.

The subproblems of the method presented in the preceding section are discretized using direct collocation.[23–25] In this approach, the state trajectories between the gridpoints are approximated by piecewise cubic polynomials. The control functions are approximated piecewise linearly. The state trajectories are required to be continuous and smooth in their first derivative. In addition, in the middle of each interval, the slopes of the state trajectories are required to coincide with the state rate at the same point.

The evader's problem (65–67) is discretized using 40 equidistant gridpoints. The discretization interval is then less than 5 s in every problem, which is considered sufficient on the basis of the experience reported in Ref. 25. The pursuer's problem (60–63) is discretized using 5, 10, and 25 points for the stages of the missile, respectively. The states and the controls are required to be continuous at $t = 3$ and 15 s. With this grid, the maximal discretization interval during the last phase is approximately 7 s, which is considered sufficiently small for a missile gliding near a quasi-stationary state. The tested denser discretization grids increase the computation time but do not produce significantly different results.

The resulting nonlinear programming subproblems are solved using the NPSOL[26] library subroutine, which is a versatile implementation of sequential quadratic programming (for example, see Ref. 27). The use of the Lagrangian merit function substantially improves the convergence of the method from an almost arbitrary infeasible initial point. To bring the decision variables into the same magnitude, the discrete state and control variables of the subproblems are scaled with the maximal value of the respective variable appearing in the initial guess.

In each example, the pursuer's initial velocity $v_{P,0}$ is fixed to 300 m/s. The pursuer's initial altitude is varied from $h_{P,0} = h_{P,\min}$ to 9000 m in 1000-m intervals. The initial heading angle of the evader is varied from $\chi_{E,0} = 0$ to 180 deg in 18-deg intervals. Here

0 deg means a head on shoot and 180 deg a tail shoot. Note that the situation is symmetrical for $\chi_{E,0} > 180$ deg.

In the selected discretization grid, $10 \times 11 = 110$ game problems are solved for each combination of $h_{E,0}$, $v_{E,0}$, and $v_{P,0}$. The iteration is terminated once the relative change in the shooting distance becomes less than 0.5%.

Example 1

First, we study a case where the evader initially flies at $h_{E,0} =$ 3000 m with the initial velocity $v_{E,0} = 400$ m/s in level flight. The shooting ranges corresponding to different initial altitudes and lateral aspect angles of the pursuer are shown in Fig. 1. Because of the assumed lateral homogeneity of the atmosphere, rotating the initial heading angle of the evader with a fixed initial position of the pursuer is equivalent to rotating the initial position of the pursuer with a fixed initial direction of the evader. In Fig. 1, the evader's initial direction is fixed along the positive x axis. Missiles fired from inside the shown manifold with the specified initial velocity will reach the aircraft regardless of the aircraft's actions, whereas missiles fired from outside do not reach an optimally escaping aircraft.

Barrier saddle point trajectories of the players, related to the points labeled A, B, and C in Fig. 1, are presented in Figs. 2, 3, and 4, respectively. The corresponding loadfactors and evader's throttle settings are presented in Fig. 5. At point A, the pursuer is initially at $h_{P,0} = 50$ m directly behind the evader, and the solution trajectories

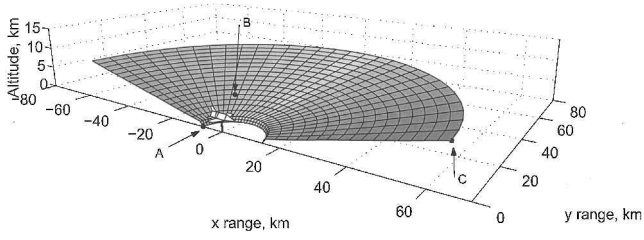

Fig. 1 Visualization of the submanifold of the barrier computed in Example 1.

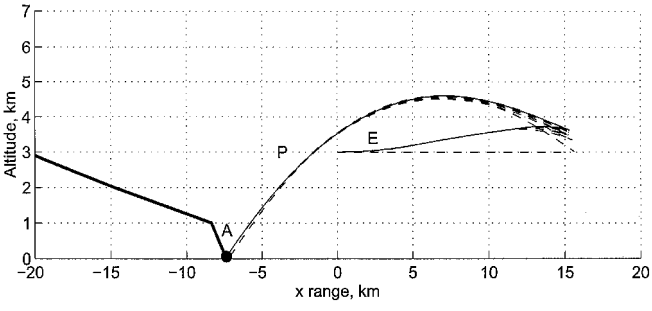

Fig. 2 Barrier trajectories of the players related to point A in Fig. 1 (——) and the convergence history of the computation (– – –); thick line represents part of the barrier submanifold.

stay in the vertical plane. The evader starts in level flight, but the dynamic pressure constraint soon forces the evader to climb. Before the capture occurs, the controls of the evader turn singular, which is indicated by the throttle setting that receives values less than 1 (see Fig. 5a). The pursuer climbs to the maximal altitude of 4.6 km and captures the evader at the altitude of 3.7 km. The initial constellation is disadvantageous for the pursuer because the shooting range is only 7.4 km. The final time is 36.7 s.

Figure 2 also shows the convergence history of the solution method. The initial guess of the evader's trajectory is a straight line in the initial altitude. Because the trajectory violates the dynamic pressure constraint, the optimal shooting range of the pursuer against this trajectory is shorter than in the other solutions. After the first iteration, the maximal shooting range decreases monotonically within the numerical accuracy. A feasible initial estimate of the evader's trajectory could be constructed by guessing the components of the gradient of $V(\cdot)$ and solving problem (65–67) once.

The 0.5% accuracy in the shooting range is achieved after four iterations, but to demonstrate the convergence we have in this example used the accuracy of 0.005%, which is achieved after nine iterations. Initiating the method with different initial trajectories for the evader leads to the same solution. The number of iterations does not heavily depend on the initial guess.

At point B, the pursuer's initial altitude is $h_{P,0} = 3000$ m, and it is 126 deg to the left of the evader's initial direction. The evader first turns away from the pursuer and climbs to avoid violating the dynamic pressure constraint and to decrease the drag force. Again, the controls turn singular in the end (Fig. 5b), but the relative duration of the singular arc is shorter. During the first 10 s, the bank angle of the evader (not plotted) is around 60 deg and decreases then in the next 10 s gradually to zero. The pursuer selects its initial heading in such a way that no lateral turning is needed, and the optimal bank angle is zero.

The pursuer climbs to the maximum altitude of 24.9 km. On one hand, climbing brings the pursuer into a thin atmosphere where the drag force is smaller than in lower altitudes. On the other hand, climbing and trading kinetic energy into potential energy seems to be the optimal way to reach the velocity of the maximal glide ratio for the coasting phase. Qualitatively similar range optimal glide trajectories for an aircraft with an engine fault have been obtained in Ref. 28. The initial position B is more advantageous for the pursuer than the position A because the shooting range grows to 21 km and the duration of the encounter to 145 s.

Point C refers to a head on shoot from $h_{P,0} = 9$ km. The initial state is on the dispersal surface of the evader, who must instantaneously decide whether to turn left or right. Here, the evader turns right, almost 180 deg, and climbs simultaneously. The pursuer climbs to the altitude of more than 34 km and then glides down to 10.5 km, where the capture occurs, flying altogether almost 150 km. The optimal bank angles of the players are similar to the preceding solution. Because of the tactically superior position of the pursuer, the shooting range is 64.9 km, and the duration of the encounter is 182 s.

A plot of the maximal shooting ranges corresponding to the pursuer's different initial altitudes and directions of shoot is presented in

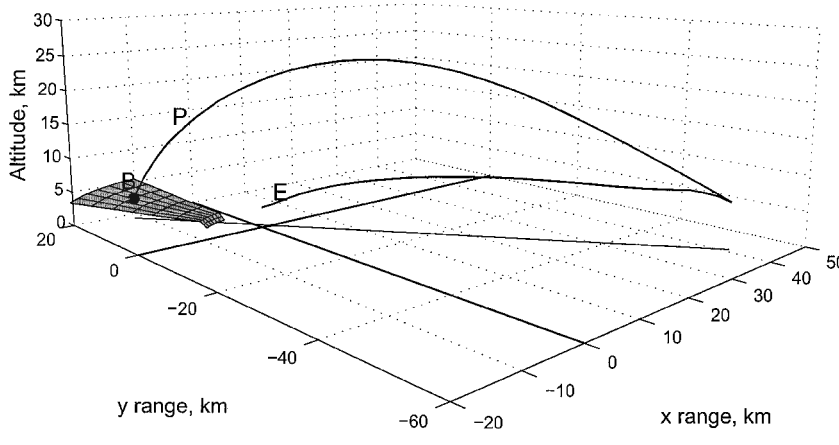

Fig. 3 Barrier trajectories related to point B in Fig. 1, together with the projections in the *xy* plane.

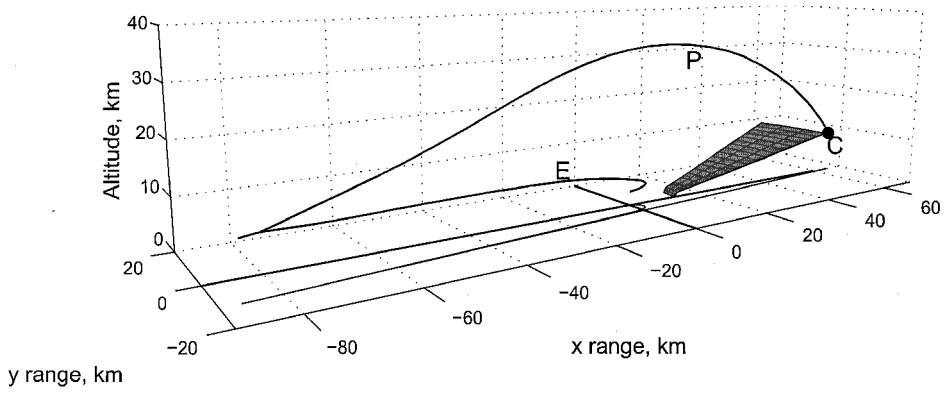

Fig. 4 Barrier trajectories related to point C in Fig. 1, together with the projections in the *xy* plane.

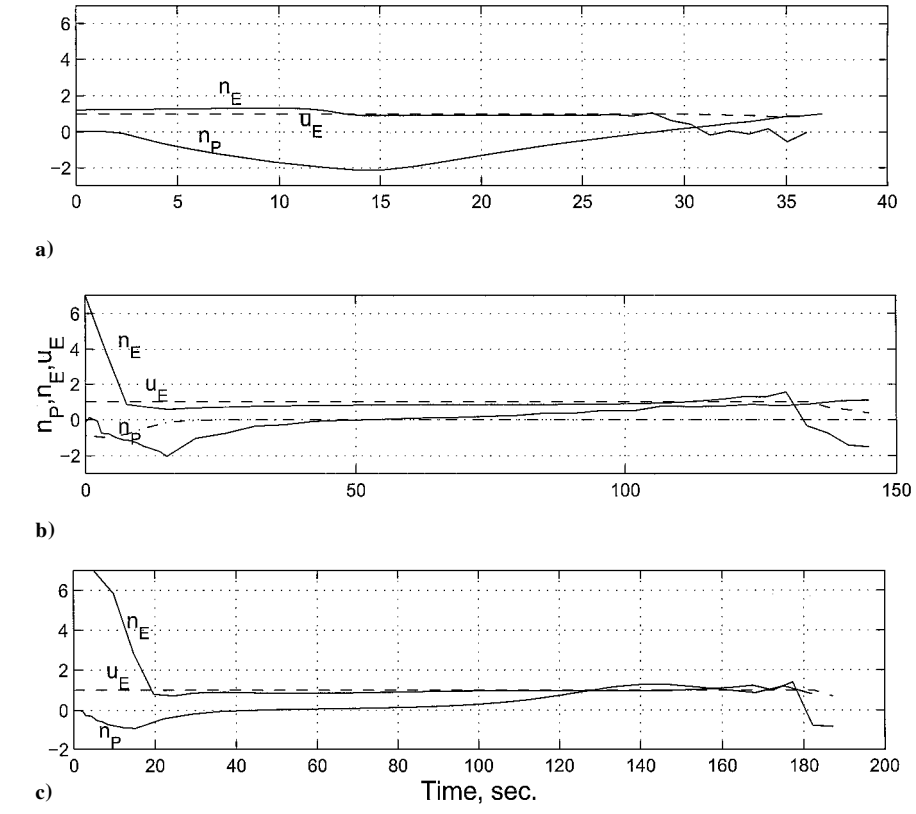

Fig. 5 Barrier saddle point loadfactors of the players (——) and the throttle setting of the evader (– – –) along trajectories related to points A, B, and C in Fig. 1.

Fig. 6. The earlier discussed points A, B, and C are also shown. The effect of the atmosphere is visible in the lower part of the manifold. When the pursuer starts from a low altitude, it stays in the denser part of the atmosphere during the flight. As a result, the maximal shooting range is relatively small. However, when the initial altitude of the pursuer increases, it can reach thinner atmosphere, and the maximal shooting range grows almost linearly with the initial total energy of the pursuer.

When the pursuer is initially in a low altitude, the maximal shooting range clearly depends on the direction of the shoot. In higher initial altitudes, however, the dependence is alleviated. An intuitive explanation is as follows. In every case, and especially in a head on shoot, the evader's optimal strategy is to turn away from the pursuer regardless of the pursuer's initial altitude, even though the turn itself does not increase the distance to the pursuer. The duration of the turn is roughly constant, whereas the terminal time increases with the initial altitude of the pursuer. Thus, with the shooting directions in front of the evader (heading angles near 0 deg) and with low initial altitudes of the pursuer, the evader uses most of the available flight time in turning, whereas in solutions corresponding to high initial altitudes of the pursuer, the fraction of the total time the evader uses for turning is smaller.

In addition to turning away from the pursuer, the evader also ascends to avoid the dynamic pressure constraint that becomes active toward the end of the encounter. The pursuer's strategy is to climb for the reasons discussed earlier. Consequently, the optimal initial flight-path angle of the pursuer is often more than 60 deg. Some comparisons indicate that constraining the initial flight-path angle and heading angle such that the target is required to be within a cone of visibility with an opening angle of 35 deg shows a decrease of the magnitude of 10% in the maximal shooting range. The difference is mainly due to the momentary but large loadfactor needed to steer the pursuer upward and laterally toward the final position of the evader. Thus, the significance of the free initial direction of the pursuer seems to be noteworthy.

Example 2

In example 2, the initial velocity of the evader is decreased to 250 m/s. The maximal shooting range is presented as a function of the pursuer's initial altitude and the direction of shoot in Fig. 7. Note

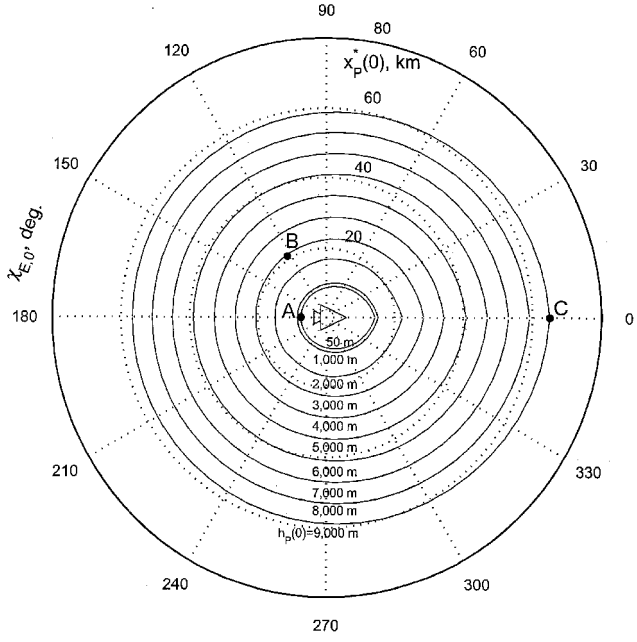

Fig. 6 Shooting range as a function of the pursuer's initial altitude and the direction of the shoot in example 1; evader lies in the origin and flies to the right.

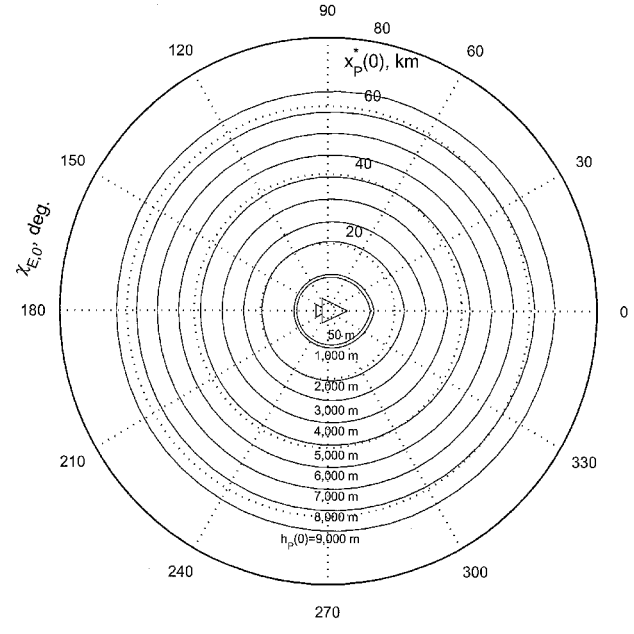

Fig. 7 Shooting range as a function of the pursuer's initial altitude and the direction of the shoot in example 2.

that with higher initial altitudes of the pursuer, the maximal shooting range grows less than 10% on the average when compared to the preceding example. One would expect that the lower initial energy of the evader would be more advantageous for the pursuer. The thrust excess, that is, the difference of the thrust force and the drag force of the evader is, however, larger with lower velocities, and acceleration to almost the same velocity as with the higher initial velocity takes only a fraction of the terminal time. The velocity difference, thus, becomes almost compensated in the first moments of the flight. In the lower parts of the barrier submanifold, the difference is larger because the acceleration takes more than half of the total flight time. On the other hand, the largest possible shooting range for a head-on shoot is smaller than in the preceding example. The turning performance of the evader is better at the lower initial velocity.

Example 3

Finally, we compute the maximal shooting ranges for an evader at $h_{E,0} = 6000$ m with the initial velocity $v_{E,0} = 400$ m/s. The maximal

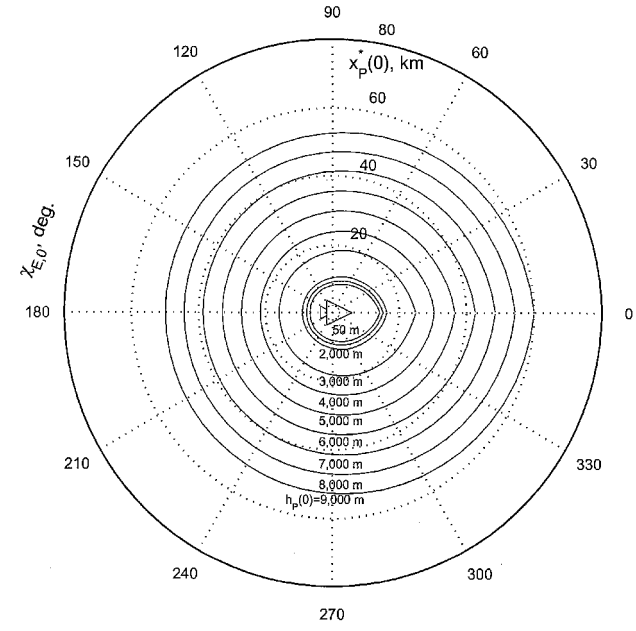

Fig. 8 Shooting range as a function of the pursuer's initial altitude and the direction of the shoot in example 3.

shooting ranges are shown as functions of the pursuer's initial altitude and the direction of shoot in Fig. 8. The higher initial altitude of the evader reduces the maximal shooting ranges. In the pursuer's initial altitudes of 2000–3000 m, the change is approximately 40% compared to the first example. In altitudes 4000 m and above, the difference varies between 10 and 15%, with 13% on the average.

Conclusions

We have presented a method to compute the capture set of a missile with given vehicle models under the assumption that both the missile and the aircraft behave in the best possible way. Instead of solving the necessary conditions of the corresponding game of kind, an equivalent game of degree is set up. A submanifold of the barrier in three dimensions is constructed by solving the game of degree repeatedly with suitably discretized initial states using a decomposition method presented earlier. The necessary conditions of the game need not be solved explicitly. The use of discretization and nonlinear programming in solving the subproblems of the decomposition offers a tradeoff possibility between accuracy and solution time. A coarse solution with only few discretization points can be obtained fast for inspection, and, if desired, can be improved by adding of reallocating the discretization points. More efficient computation could be achieved with optimization algorithms designed especially for sparse problems and possibly parallelization.

The presented demonstrations show, as expected, that the maximal shooting range depends on the altitude difference of the players and, through the properties of the atmosphere, also on the absolute initial altitude of the pursuer. The shape of the lower part of the no escape envelope depends largely on the direction of the shoot, but in the upper part this dependence is diluted.

The computations indicate that the shooting range is rather insensitive to small changes in the evader's trajectory. On one hand, this means that a successful implementation of the evasive maneuvers is not crucially affected by small variations. On the other hand, because the maximization in the presented decomposition method is essentially a first-order approach, it may suffer from convergence difficulties near such a flat optimum. Nonetheless, as pointed out in Ref. 18, the maximization problem can be solved using any method of nonlinear programming, including second-order algorithms. Another possibility to obtain more accurate results is to initiate an indirect solution method with the obtained solution. The initial estimate of the adjoint variables can be calculated using the Lagrange multipliers of the converged subproblems.

The approach provides a way to assess the technical performance of the vehicles in the worst possible case, which is important

especially if the guidance law of the missile is unknown. It should be noted, however, that in this paper the information pattern is unmodeled and assumed perfect. Usually it is the aircraft that has problems in receiving information on the missile. For example, detecting a missile launch is a challenging task. If a missile can hide itself, the largest possible shooting range thus becomes larger.

Acknowledgment

This work has been carried out in collaboration with the Finnish Air Force.

References

[1]Shinar, J., Guelman, M., and Green, A., "An Optimal Guidance Law for a Planar Pursuit–Evasion Game of Kind," *Computers and Mathematics with Applications*, Vol. 18, No. 1–3, 1989, pp. 35–44.

[2]Grimm, W., and Schaeffer, J., "Optimal Launch Conditions on the No-Escape Envelope," *Computers and Mathematics with Applications*, Vol. 18, No. 1–3, 1989, pp. 45–59.

[3]Isaacs, R., *Differential Games,* reprint, Krieger, New York, 1975.

[4]Blacquire, A., *Quantitative and Qualitative Games,* Academic, New York, 1969, Chap. 6.

[5]Imado, F., and Miwa, S., "Fighter Evasive Maneuvers Against Proportional Navigation Missile," *Journal of Aircraft*, Vol. 23, No. 11, 1986, pp. 825–830.

[6]Imado, F., and Miwa, S., "Fighter Evasive Boundaries Against Missiles," *Computers and Mathematics with Applications*, Vol. 18, No. 1–3, 1989, pp. 1–14.

[7]Imado, F., "Some Aspects of a Realistic Three-Dimensional Pursuit-Evasion Game," *Journal of Guidance, Control, and Dynamics*, Vol. 16, No. 2, 1993, pp. 289–293.

[8]Shinar, J., and Guelman, M., "New Results in Optimal Missile Avoidance Analysis," *Journal of Guidance, Control, and Dynamics*, Vol. 17, No. 5, 1994, pp. 897–902.

[9]Ong, S., and Pierson, B., "Optimal Planar Evasive Aircraft Maneuvers Against Proportional Navigation Missiles," *Journal of Guidance, Control, and Dynamics,* Vol. 19, No. 6, 1996, pp. 1210–1215.

[10]Zarchan, P., "Proportional Navigation and Weaving Targets," *Journal of Guidance, Control, and Dynamics*, Vol. 18, No. 8, 1995, pp. 969–974.

[11]Imado, F., and Miwa, S., "Missile Guidance Algorithm Against High-*g* Barrel Roll Maneuvers," *Journal of Guidance, Control, and Dynamics*, Vol. 17, No. 1, 1994, pp. 123–128.

[12]Kumar, R., Seywald, H., and Cliff, E., "Near-Optimal Three Dimensional Air-to-Air Missile Guidance Against Maneuvering Target," *Journal of Guidance, Control, and Dynamics*, Vol. 18, No. 3, 1995, pp. 457–464.

[13]Green, A., Shinar, J., and Guelman, M., "Game Optimal Guidance Law Synthesis for Short Range Missiles," *Journal of Guidance, Control, and Dynamics*, Vol. 15, No. 1, 1992, pp. 191–197.

[14]Le Menec, S., and Bernhard, P., "Decision Support System for Medium Range Aerial Duels Combining Elements of Pursuit-Evasion Game Solutions with AI Techniques," *New Trends in Dynamic Games and Applications,* edited by G. J. Olsder, Birkhäuser, Boston, 1995, pp. 207–226.

[15]Breitner, M., Pesch, H., and Grimm, W., "Complex Differential Games of Pursuit–Evasion Type with State Constraints, Part 1: Necessary Conditions for Optimal Open-Loop Strategies," *Journal of Optimization Theory and Applications*, Vol. 78, No. 3, 1993, pp. 419–441.

[16]Breitner, M., Pesch, H., and Grimm, W., "Complex Differential Games of Pursuit–Evasion Type with State Constraints, Part 2: Numerical Computation of Optimal Open-Loop Strategies," *Journal of Optimization Theory and Applications*, Vol. 78, No. 3, 1993, pp. 443–463.

[17]Raivio, T., and Ehtamo, H., "On Numerical Solution of a Class of Pursuit-Evasion Games," *Annals of the International Society of Dynamic Games*, Vol. 5, 2000, pp. 177–201.

[18]Ehtamo, H., and Raivio, T., "On Applied Nonlinear and Bilevel Programming for Pursuit–Evasion Games," *Journal of Optimization Theory and Applications* (to be published).

[19]Raivio, T., and Ehtamo, H., "Visual Aircraft Identification as a Pursuit-Evasion Game," *Journal of Guidance, Control, and Dynamics*, Vol. 23, No. 4, 2000, pp. 701–708.

[20]Lachner, R., Breitner, M., and Pesch, H. J., "Three-Dimensional Air Combat: Numerical Solution of Complex Differential Games," *Annals of the International Society of Dynamic Games*, Vol. 3, 1996, pp. 165–190.

[21]Betts, J., "Survey of Numerical Methods for Trajectory Optimization," *Journal of Guidance, Control, and Dynamics*, Vol. 21, No. 2, 1998, pp. 193–207.

[22]Shimitsu, K., Ishizuka, Y., and Bard, J., *Nondifferentiable and Two-Level Mathematical Programming*, Kluwer Academic, Boston, 1997, Chap. 9.

[23]Hargraves, C. R., and Paris, S. W., "Direct Trajectory Optimization Using Nonlinear Programming and Collocation," *Journal of Guidance, Control, and Dynamics*, Vol. 10, No. 4, 1987, pp. 338–342.

[24]von Stryk, O., and Bulirsch, R., "Direct and Indirect Methods for Trajectory Optimization," *Annals of Operations Research*, Vol. 37, 1992, pp. 357–373.

[25]Raivio, T., Ehtamo, H., and Hämäläinen, R. P., "Aircraft Trajectory Optimization Using Nonlinear Programming," *System Modeling and Optimization*, edited by J. Dolezal and J. Fidler, Chapman and Hall, London, 1996, pp. 435–441.

[26]Gill, P., Murray, W., Saunders, M., and Wright, M., "User's Guide for NPSOL 4.0: A Fortran Package for Nonlinear Programming," Stanford Univ., Rept. SOL 86-4, Stanford, CA, 1986.

[27]Bertsekas, D., *Nonlinear Programming*., Athena Scientific, Belmont, MA, 1995, Chap. 4.

[28]Hoffren, J., and Raivio, T., "Optimal Maneuvering After Engine Failure," *Proceedings of the 2000 AIAA Flight Mechanics Conference,* AIAA, Reston, VA, 2000, pp. 277–287.